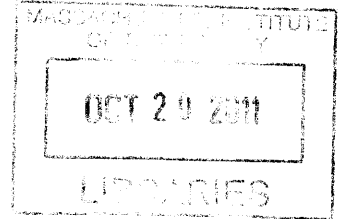


Mechanical Development of the Actuation System  
of a Parabolic Solar Trough

by

Conor R. O'Rourke



Submitted to the  
Department of Mechanical Engineering  
in Partial Fulfillment of the Requirements for the Degree of

**ARCHIVES**

Bachelor of Science

at the

Massachusetts Institute of Technology

June 2011

© 2011 Conor R. O'Rourke  
All rights reserved

The author hereby grants to MIT permission to reproduce and to  
distribute publicly paper and electronic copies of this thesis document in whole or  
in part in any medium now known or hereafter created.

Signature of Author.....  
Department of Mechanical Engineering  
May 6, 2011

Certified by.....  
Alexander H. Slocum  
Neil and Jane Pappalardo Professor of Mechanical Engineering  
Thesis Supervisor

Accepted by.....  
John H. Lienhard V  
Samuel C. Collins Professor of Mechanical Engineering  
Undergraduate Officer



# Mechanical Development of the Actuation System of a Parabolic Solar Trough

by

Conor R. O'Rourke

Submitted to the Department of Mechanical Engineering  
in partial fulfillment of the requirements for the degree of  
Bachelor of Science in Mechanical Engineering

## **Abstract**

This thesis documents my personal contribution to the engineering and design of an actuation system with the purpose of rotating a parabolic solar trough to track the sun throughout the day. The primary focus of the design was to create a robust system with minimal cost while meeting a number of functional requirements. After considering a number of possible designs and conducting an in-depth analysis into two of them, the final design chosen was a slider crank mechanism that rotates the trough about its focus. This mechanism uses a lead screw to drive the base of two passively extensible arms in a lateral direction and translates that force into a rotational motion. Whichever arm is in compression actuates the trough. One of these bases is driven by the lead screw while the other is fixed a distance away using a rigid connection. The model for this system was optimized for cost and design simplicity resulting in the selection and purchase of parts for a full scale prototype at a site in New Hampshire using one 4ft lead screw and a 0.16 horsepower motor to drive each end of the trough.

Thesis Supervisor: Alexander H. Slocum

Title: Neil and Jane Pappalardo Professor of Mechanical Engineering

## **Acknowledgements**

First I would like to thank my advisor, Alex Slocum for his guidance and knowledge as well as Sandy Campbell for also being there and helping our team through the design process. Your help has been invaluable and has taught me so much about the engineering process. Secondly, I would like to thank my teammates Eric Gilbertson and Tim Robertson. This project would have been impossible without your help and you being there to bounce ideas off of. Lastly, I would like to thank my friends and family for being there throughout this arduous semester.

# Table of Contents

Abstract.....	3
Acknowledgements.....	4
I. Introduction.....	9
1.1 Goals.....	9
1.2 Functional Requirements.....	9
1.3 Existing Design .....	13
1.3.1 Background .....	13
1.3.2 Trough Structure.....	13
1.3.3 Actuation System and Primary Failure Mode.....	14
II. Conditions Modeling .....	15
2.1 Torque.....	15
2.2 Sun Insolation and Shading Due to the Mechanism .....	17
2.2.1 Tracking the Sun .....	18
2.2.2 Results .....	21
III. Concept Development.....	23
3.1 Early Concepts .....	23
3.2 Double Slider Crank Concept.....	23
3.2.1 Description .....	23
3.2.2 Geometric Analysis.....	25
3.2.3 Analysis and Optimization .....	27
3.2.4 Primary Failure Modes.....	29
3.3 Twin Four-Bar Concept .....	30
3.3.1 Description .....	30
3.3.2 Geometric Analysis.....	31
3.3.3 Actuator Speed and Length .....	32
3.3.4 Analysis and Optimization .....	33
3.3.5 Primary Failure Modes.....	36
3.4 Manufacturing Design and Costing.....	36
3.4.1 Slider Crank Manufacturing Design.....	36
3.4.2 Twin-Four Bar Manufacturing Design.....	39
3.4.3 Cost Comparison .....	40

IV. Final Design and Full Scale 4m Prototype .....	41
4.1 Selection of Slider Crank .....	41
4.2 Improved Slider Crank Design.....	41
4.3 Part Design and Selection .....	44
4.3.1 Linear Guide .....	44
4.3.2 Screw Coupling .....	44
4.3.3 Other Couplings and Materials Selection .....	45
V. Further Work.....	46
VI. References .....	47

## List of Figures

Figure 1: Bulkhead and ring system as designed prior to the current semester's work.....	14
Figure 2: Drive system design from April 12, 2010.....	14
Figure 3: Normal and failure mode effective radii and resultant force directions for the original chain drive system. ....	15
Figure 4: Physical variables used for all torque calculations. ....	16
Figure 5: Torque [Nm] across one half of the trough's movement cycle.....	17
Figure 6: Illustration of the effect of the sun elevation angle on the distribution of insolation.....	18
Figure 7: Percentage insolation loss as the average width of the actuation system increases, keeping the height fixed at 1.8m. ....	22
Figure 8: Visualization of two states of the slider-crank system when the right arm is driving. ....	24
Figure 9: Illustration of possible slotted connection aimed to decrease likelihood of failure when arms transition the load.....	25
Figure 10: Visualization of physical dimensions R, H, L, d and $\tau$ used in slider-crank calculations.....	26
Figure 11: Second boundary condition, where the driving arm is vertical, and the case to show the total length of lead screw for slider-crank concept.....	27
Figure 12: Torque response surface shows the maximum torque throughout the entire 110° cycle for any given pair of R and H. Highlighted is the chosen value of approximately R=0.16m and H=1.55m resulting in a maximum torque of approximately 83 Nm assuming a lead of 10 threads/inch and $\eta=0.5$ .....	28
Figure 13: Screw length response surface using the same parameters as above.....	28
Figure 14: A general illustration of the twin four-bar concept.....	30
Figure 15: Visualization of physical dimensions R, H, $D_A$ and $\beta$ used in twin four-bar concept calculations. ....	31
Figure 16: Actuator velocity vs. trough angle for the twin four-bar actuators.....	33

Figure 17: Twin four-bar actuator lengths and compression ratios only shown for ratios between 1.3 and 1.8.  $\theta=35^\circ$ . ..... 34

Figure 18: Twin four-bar force response surface showing that the maximum force required to rotate the trough increases exponentially as the pinned point approaches the center of the trough.  $\theta=35^\circ$ . ..... 35

Figure 19: Simple SolidWorks model of the slider crank concept. At this point the left arm is driving the trough while the right arm extends. .... 37

Figure 20: Example of the slider crank trolley acting as a linear guide on an I-beam. .... 38

Figure 21: Close up of a rough SolidWorks model of the twin four bar design. .... 39

Figure 22: Preliminary custom screw coupling for slider crank design shown with half of the trolley assembly. .... 45



# **I. Introduction**

## **1.1 Goals**

The goal of this project is to design, evaluate, and prototype an actuation system for a solar collection trough to meet the specified functional requirements. There has already been preliminary work on designing the structure of the trough as well as an actuation system. The current actuation system has a design failure mode that causes its chain actuation mechanism to fail prematurely and at the same time causes too much shadowing loss, so another must be designed.

## **1.2 Functional Requirements**

The project is funded by Eni, an Italian oil and gas company, and will potentially be used in Tunisia to preheat water or oil for use in another process. The primary competition for this design is a design by Eurotrough which produces a solar trough that uses glass mirrors and is rotated about its center of mass behind the trough. The functional requirements are primarily based on directions from Eni as well as metrics of the Eurotrough.

### 1) +/- 110 degrees of motion

This is a requirement by Eni so that the trough can be moved to a stored position in the event of adverse environmental conditions. These troughs are being designed to be installed in an array in a hot desert climate. This means that the troughs may have to withstand sand storms or heavy wind loads. By allowing the trough to actuate to 110 degrees, the trough will be able to face away from heavy winds in an aerodynamic position.

## 2) Rotate trough about parabola focus point

This is one of the distinguishing features compared to the competition, Eurotrough. The purpose of these troughs is to focus sunlight onto a pipe located at the focus. By flowing oil or water through that pipe, it is possible to capture the sun's energy in the fluid. By rotating the trough about the focus, this pipe does not have to move as the trough tracks the sun. This minimizes fatigue and cuts the cost of expensive rotating couplings. This failure case could result in a spill of hot oil which is highly undesirable. The Eurotrough design actuates its trough about the assembly's center of mass located behind the trough. This cuts the amount of energy required to actuate the trough, but requires much more robust couplings to link the fluid pipes, creating a potential point of failure in the trough's most critical component. A fault in one of the pipes could disrupt an entire array of troughs when they are linked in series.

## 3) 30-Year Lifetime

This is a design requirement set forth by the sponsor, Eni. As the lifetime of the mechanism increases, the marginal cost of the system per unit of energy produced decreases. As lowering costs is one of the primary goals of this project, lifetime is an important factor.

## 4) Approximately 11,000 cycles exposed to a hot desert climate

The design is being designed to withstand its 30 year lifetime in a hot desert climate. For this reason, conditions such as sand, wind, heat and others must be taken into account when choosing the design and materials. Heat, sand and moisture can be detrimental on mechanisms. The cycle estimate comes from assuming it goes through one cycle per day for 30 years.

#### 5) Angular accuracy due to linkage mechanism

<0.1 degrees during first 80 degrees of motion

<2.0 degrees in final 30 degrees of motion

Errors in the angle of the trough result in losses, so the angular accuracy must be accurate between 0 and 80 degrees, the primary range of angles at which the trough can capture sunlight. The final 30 degrees of motion are solely for storing the trough during harsh weather conditions, so accuracy is not an important factor. To evaluate the structure, mechanism, and environmental conditions such as wind must be considered. At the same time, there will be a closed loop control system monitoring the angle of the trough at any given time. This will ensure most of the accuracy as long as the actuation system is capable of reaching that point.

#### 6) Lower cost than Euro-Trough design

The primary feature of this design is that it will be more cost effective than the competing design by Euro-Trough. Euro-Trough uses hydraulic actuators to rotate their arrays. These systems are more expensive than the proposed MIT design, but they also drive much longer segments of trough decreasing their cost per solar collection area. The MIT design will focus on cutting costs in a number of places in addition to the actuation system design documented in this thesis. Paired with other cost savings, to make this project financially desirable the actuation system should cost approximately \$2000 per 12m trough. [1]

#### 7) Actuate both ends of solar trough

The trough design being designed by another MIT group has a low torsional rigidity. If driven only by one end, the weight of the materials would cause the trough to torque decreasing its efficiency. Using supported beam bending theory, rotating the trough by both ends, its maximum deflection at the center of the trough will be approximately 16 times less than the deflection at the unsupported end if it were only supported by one end.

### 8) Achieve stowed position in 2 minutes

This stowing speed is a requirement for the prototype that is partially built in New Hampshire, not for the final design. The time needs to be fast enough to facilitate testing so the engineers evaluating the design will not spend all day to examine a single cycle. The only difference this makes in the final design is the horsepower of the actuator motors. When the speed is reduced to only require enough power to track the sun (or possibly somewhat quicker in case of a storm) the design will require a lower powered, lower cost motor.

### 9) Prototype Requirement: Mate to existing design

Once the method of actuation is chosen and the prototype designed, it will be built at full scale to actuate an existing 4m prototype trough in New Hampshire. For this reason, our prototype must take into account the existing design so it can be tested. The existing actuation design relied on a bicycle chain lashed around a ring. The ring was rigidly fixed to the trough and was centered on the focal point. The ring on each end was supported by four wheels, bearing the weight of the trough and allowing it to roll, rotating the trough about the parabola's focus.

## **1.3 Existing Design**

### **1.3.1 Background**

In February 2011, when the current team inherited this project, there had already been a large amount of work done designing the trough and actuation systems. Studies were done into aerodynamics, production of the mirrored surfaces, materials used, fabrication methods, and more. One of its distinguishing factors is that it called for the use of rolled steel plates coated with a reflective film to act as the reflectors. These panels are only slightly less effective than the curved glass panels used in Eurotrough at a fraction of the cost. [1]

### **1.3.2 Trough Structure**

The first prototype was made using a number of bulkheads including one at either end of the trough which acted as supports and as attachment points for the actuation system. The bulkheads were designed to increase the stiffness of the trough while still being light and accurately produced. A steel ring bent into a circle was attached to each of the end's bulkhead. The rings acted as the support for each 12m trough. An example of what the bulkhead and ring look like can be seen in Figure 1: Bulkhead and ring system as designed prior to the current semester's work. The ring was supported by four guide wheels positioned on the base structure that allowed the system to roll about the focus of the trough. Ideally, in the final design this ring will be excluded per request from Eni and to eliminate shading of the trough's mirrors when the sun is angled the end of the trough.

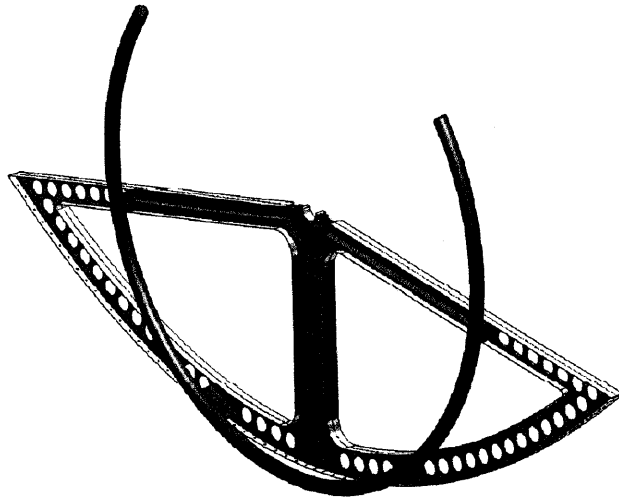


Figure 1: Bulkhead and ring system as designed prior to the current semester's work. [2]

### 1.3.3 Actuation System and Primary Failure Mode.

The actuation system used a roller chain attached to the ring to pull the trough along guide wheels. At either end of the roller, the chain was tensioned while the motor is looped through a set of gears at the lowest point of the roller as shown in Figure 2: Drive system design from April 12, 2010..

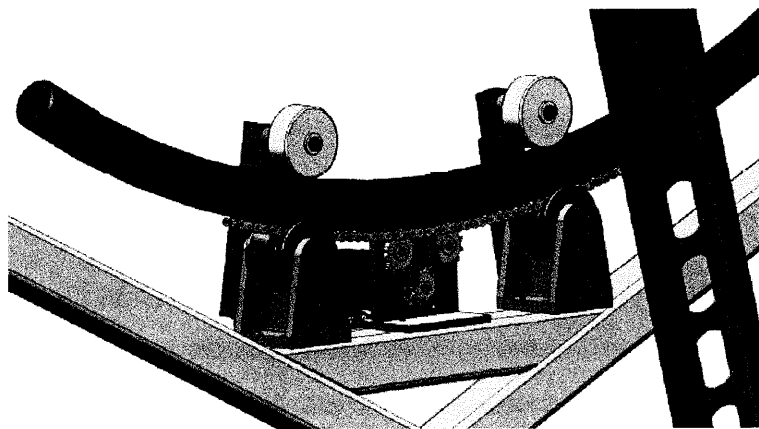


Figure 2: Drive system design from April 12, 2010. [2]

Even though the chain was tensioned at the ends, over time the chain on the prototype stretched and became loose. Since it was only secured to the ring at the ends, the chain no longer stayed against the ring, adding an unacceptable level of slack and potentially causing the system to fail. If the chain slides off of the ring, the resultant motor force would no longer be pulling in a tangential direction and the effective lever arm would be greatly decreased as seen in Figure 3. This is the primary failure mode of this actuation system. In this case, the motor would likely not have enough power to rotate the trough, damaging it in the process.

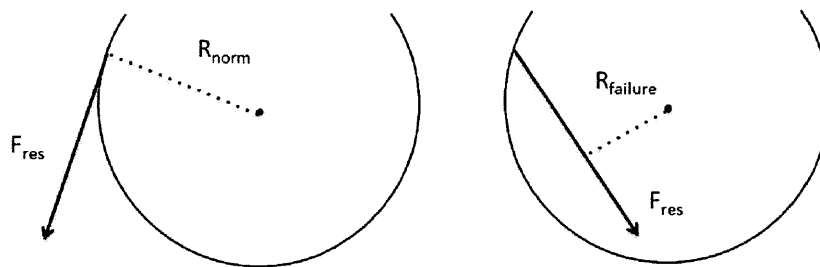


Figure 3: Normal and failure mode effective radii and resultant force directions for the original chain drive system.

## II. Conditions Modeling

### 2.1 Torque

Understanding the torque required to actuate the trough is important when designing the structure and determining the power requirements of the actuation system. Modeled as a static system, the required torque at any position is a function of gravitational forces and wind loading. This model is used later to analyze the torque and power required by the competing designs.

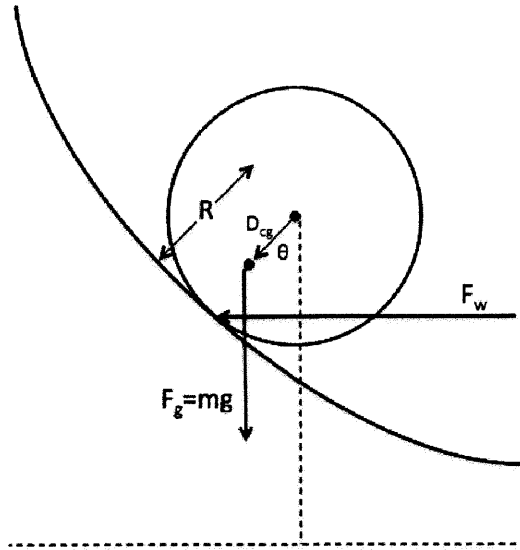


Figure 4: Physical variables used for all torque calculations.

The net torque can be expressed as below, the first term being the gravitational component and the second being the wind load.  $m$  is the mass of the rotating portion of the solar trough,  $g$  is the acceleration due to gravity,  $D_{cg}$  is the distance between the focal length and the center of mass,  $\theta$  is the angle of the trough with respect to facing vertical,  $\rho$  is the density of air,  $A$  is the planar face area of the trough,  $R$  is the focal length of the trough,  $C$  is the drag coefficient of the trough, and  $v$  is the velocity of wind.

$$\Gamma = mgD_{cg} \sin \theta + \frac{1}{2} \rho A R C v^2 \sin \theta \cos \theta$$

For the 4m prototype trough design, the following parameters were used for torque calculations. 15 m/s is the maximum operating wind speed at the proposed installation location in Tunisia. [3]



Parameter	Value
m	350kg
$\rho$	1kg/m <sup>3</sup>
A	22.8m <sup>2</sup>
R	1.7m
C	1.2
v	15m/s
D <sub>cg</sub>	1m

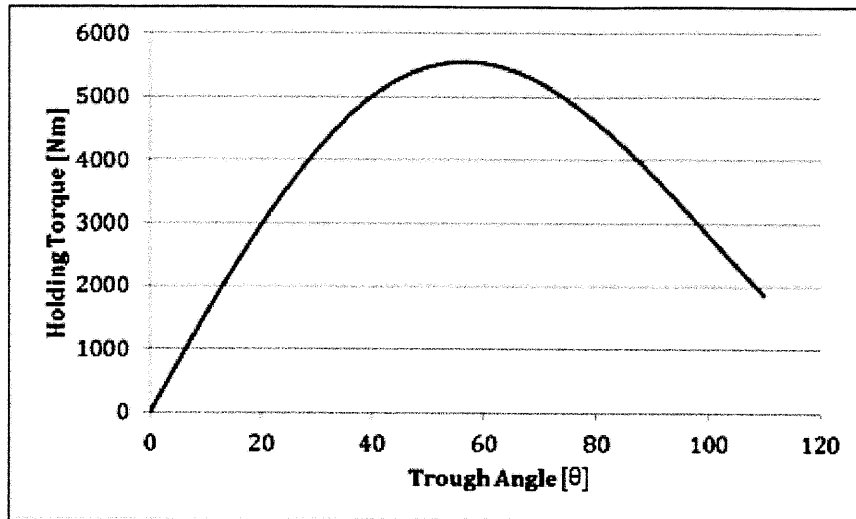


Figure 5: Torque [Nm] across one half of the trough's movement cycle. [θ]

## 2.2 Sun Insolation and Shading Due to the Mechanism

To understand the costs and benefits of adding mechanisms that would shade the reflective surface, an understanding of how the sun moves throughout the year is required. Due to the eccentricity of its orbit and its axial tilt, the angle at which the sun crosses the sky changes throughout the day and the year. In a simple understanding, these are the reasons why the seasons change and days get longer and shorter throughout them. The angle of the sun will affect the collecting potential of the solar trough as well as the amount of shade any mechanism above the trough will shade the reflective panels.

### 2.2.1 Tracking the Sun

First, to maximize the amount of insolation that the trough can receive, the trough is actuated to track the sun as it moves from the east to the west throughout the day. This actuation system is the goal of this project. In this analysis we can ignore losses due to the sun not directly facing the trough in the east/west direction because the actuation system will track it in this direction. This is not true in the north/south direction. As the seasons change, the sun can rise and set to the north or south of the trough, causing the sunlight to strike the trough at an angle, decreasing the effective collection area of the trough.

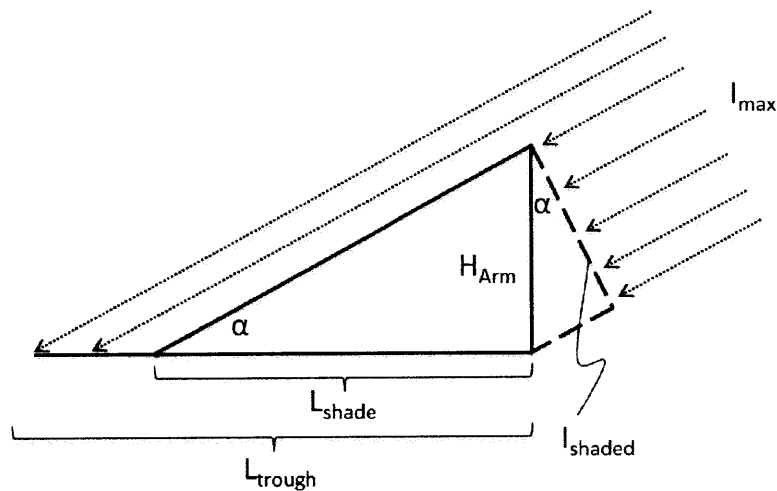


Figure 6: Illustration of the effect of the sun elevation angle  $\alpha$  on the distribution of insolation.

The angle from north to south that the sun reaches the trough at decreases the effective insolation area to:

$$A_{collection} = A_{trough} * \sin(\alpha)$$

The shading area is in the vertical direction and its area component on the trough face can be described by the equation below where,  $H_{act}$  is the height of the actuation system,  $A_{act}$  is the planar area of the actuation and support system that blocks incoming sun from the side, and  $W_{avg} = A_{act}/H_{act}$ . The second case in the

expression below describes the case when the shadow of the actuation system reaches past the end of the trough.

$$A_{shade} = \begin{cases} A_{actuator} * \cos(\alpha), & x < 0 \\ W_{avg} * L_{trough} * \sin(\alpha), & \frac{H_{act}}{\tan(\alpha)} \geq L_{trough} \end{cases}$$

Using these relations the simplified calculation for the percentage energy loss due to shading can be shown as below,

$$\% \text{ Shading Loss} = \int_{year} \left[ \frac{A_{shade}}{A_{collection}} \right] dt$$

The difficult part now is to calculate the angle and number of hours it is above head throughout the course of the year.

In astronomy, this angle  $\alpha$  is called the elevation of the sun, measured in degrees. At sunrise and sunset,  $\alpha$  is equal to zero as it crosses the horizon. This angle reaches its maximum at exactly noon local solar time. Local solar time takes into account the location of the solar trough, because time zones span many miles of longitude causing a discrepancy between local time and local solar time. There are a number of equations that eventually result in the ability to calculate the elevation of the sun throughout the day and the year. [4]

The Equation of Time (EoT) adjusts the local solar time in minutes according to the eccentricity of the earth's orbit and its tilt relative to the sun where  $d$  is the day of the year measured continuously from 0 to 365.25.

$$EoT = 9.87 \sin(2B) - 7.53 \cos(B) - 1.5 \sin(B)$$

Where:

$$B = \frac{360}{365} (d - 81)$$

The local solar time takes into account the adjustments of the EoT as well as the time zone and longitudinal location of the trough where LT is the local time.

$$LST = \frac{1}{15} [15^\circ * \Delta T_{GMT} - longitude] + EoT$$

The declination angle of the sun, a measure of the tilt of the earth relative to the sun's incoming rays, can be expressed as:

$$\delta = 23.45 \sin \left[ \frac{360}{365} (d - 81) \right]$$

The locational variables for Tunisia, assuming at the capital, are the following:

$$\Delta T_{GMT} = +1:00 \text{ hr}$$

$$Latitude = \varphi = 36.85^\circ N$$

$$Longitude = 10.15^\circ E$$

The time of the day represented by an angle,  $0^\circ$  being at noon, is represented by the hour angle (HRA) calculated knowing that the sun rotates  $360^\circ$  throughout each 24 hour period.

$$HRA = 15^\circ (LST - 12)$$

The number of hours of sunlight in a day can be calculated according to the locational variables and time. Sunrise is half of this time before 12pm and sunset is half of this time after 12pm.

$$\begin{aligned} HRS &= \frac{2}{15^\circ} \cos^{-1} \left[ \frac{-\sin(\varphi) \sin(\delta)}{\cos(\varphi) \cos(\delta)} \right] - \frac{1}{15} [15^\circ * \Delta T_{GMT} - longitude] - \frac{EoT}{60} \\ &= \frac{2}{15^\circ} \cos^{-1} [-0749 \tan(\delta)] - \frac{19.4 + EoT}{60} \end{aligned}$$

To evaluate the amount of insolation we need to integrate the amount of insolation on the trough as the elevation varies throughout the day and then sum up each of these days throughout the year. When calculating HRS, the integer of  $d$  is used to make the integral definite, while when calculating  $\alpha$  a time of  $d + t/24$  was used so that the angle would vary throughout the day. Without shading, the equation is the same except without the  $A_{arm}$  portion.

$$Effective\ Insolation\ Area = \sum_{d=0}^{d=365} \int_{12-HRS/2}^{12+HRS/2} [A_{collection} - A_{shade}] dt$$

### 2.2.2 Results

With a fixed height of 1.8m, approximately the minimum required height of the system to support the trough at the focal point, the percentage insolation loss as a factor of the average width of the actuation system. The losses increase linearly as the area of the actuation system increases. If the latitude, longitude, and elevation of the trough site were to be changed, the slope of this line would also change. These numbers are unique for a 12m trough and the latitude and longitude given in the previous section, which correspond to a location in Tunisia.

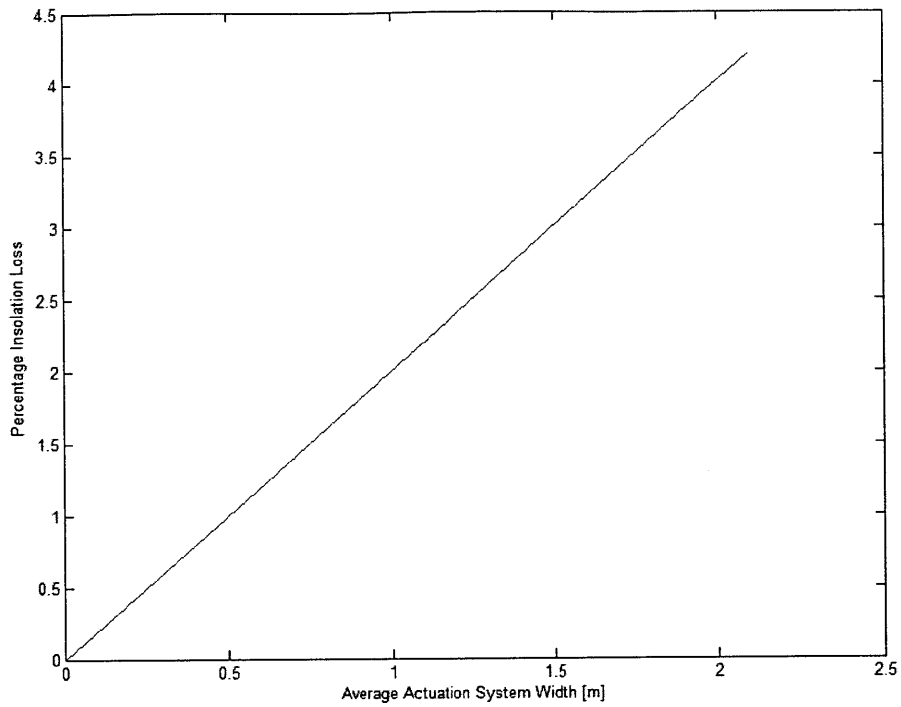


Figure 7: Percentage insolation loss as the average width of the actuation system increases, keeping the height fixed at 1.8m.

To keep this shading less than a 1% loss, the area of the kingpost, structured support, slider mechanism, and arms above the parabolic surface must be less than an average of 0.9 square meters.

## **III. Concept Development**

### **3.1 Early Concepts**

At this stage, we were not yet familiar with the existing design or direction of the structural team. Eric, Tim and I brainstormed a number of ideas for the actuation and mounting system. We were informed later that the structural team was already planning on having a king post that would rise up vertically from the ground to support the trough. The trough would then have a single arm, possibly supported in a more robust manner towards its base. Some of the early concepts did not use this design. After evaluating these ideas, we eventually settled on analyzing two concepts in detail, a double slider crank and a twin four-bar linkage.

### **3.2 Double Slider Crank Concept**

#### **3.2.1 Description**

The proposed design uses a double slider crank. Two arms are incorporated so the driving arm never has to pass through a singularity, locking up the system. The arms are pinned a distance  $R$  from the focal point and are attached to a ball screw at the bottom. The screw, driven by a small motor, drives these bases linearly, translating the force through the bars and providing all the force needed to rotate the trough. The structure of the parabola acts as the second arm of the linkage. With the second arm constrained to rotate about the focus and the first arm being driven linearly, the point of connection is rotated in a circle about the focus.

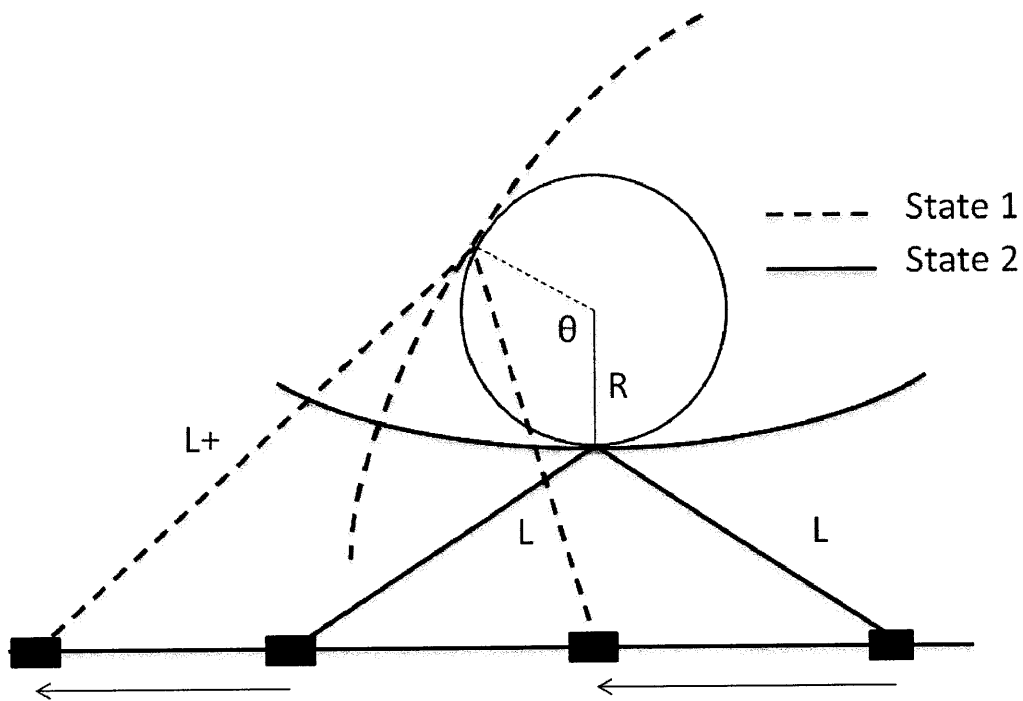


Figure 8: Visualization of two states of the slider-crank system when the right arm is driving, showing  $R = \text{focal length}$ .

To prevent singularities in the system, each arm bears the entire load for either the positive or negative angles of tilt. As seen in Figure 8: Visualization of two states of the slider-crank system when the right arm is driving, the right arm is bearing the load when the trough is being rotated up and to the left. The right arm is already past its singularity point, so it can force the trough to  $110^\circ$  without difficulty. When this arm is bearing load, the left arm bears none. Its base translates at the same rate as the right end base.

Due to the geometry of the system, keeping the bases a fixed distance apart would require the non-loaded arm to extend otherwise it would over constrain the system. For this reason, the arms have been designed to be telescoping by nesting one tube in another. They each have a minimum compressed length, which they will reach when applying force, but when they are pulled on, the inner tube will partially slide out to whatever length the system requires. By solving this problem with a passive mechanical system, it negates the need for control systems to coordinate the



rate of two separate lead screws to drive the arms as well as the cost of that more elaborate system. When the angular deflection of the trough is zero, each arm will be at the minimum length. This is where the transition between which arm is bearing the load occurs. A proposed addition to the design is a slotted connection where the two arms attach to the trough and pivot. This design latitude built into the connection should be sufficient to avoid failure from sources of variance during the transition between the arms bearing the load. The slot would most likely look somewhat like Figure 9. Since the trough will not be moving during the transition point, the vertical displacement of this point will not be changing as seen between the first two states in Figure 9.

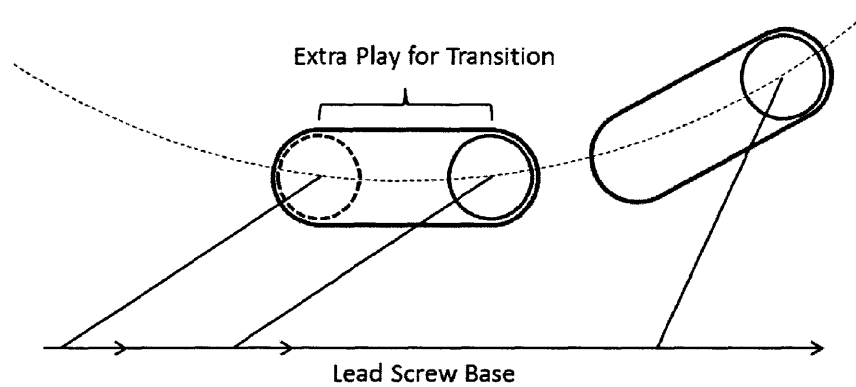


Figure 9: Illustration of possible slotted connection designed to increase design robustness when arms transition the load.

### 3.2.2 Geometric Analysis

To optimize the system, we analyzed the effect of varying the lever arm radius between the focal point and point of attachment, as well as the distance between that connection point and the lead screw. These variables are  $R$  and  $H$  respectively. By designating two boundary conditions, we can calculate the motor torque, arm length  $L$ , and length of lead screw required for any set of  $R$ ,  $H$  and angle  $\theta$  the trough might be at.

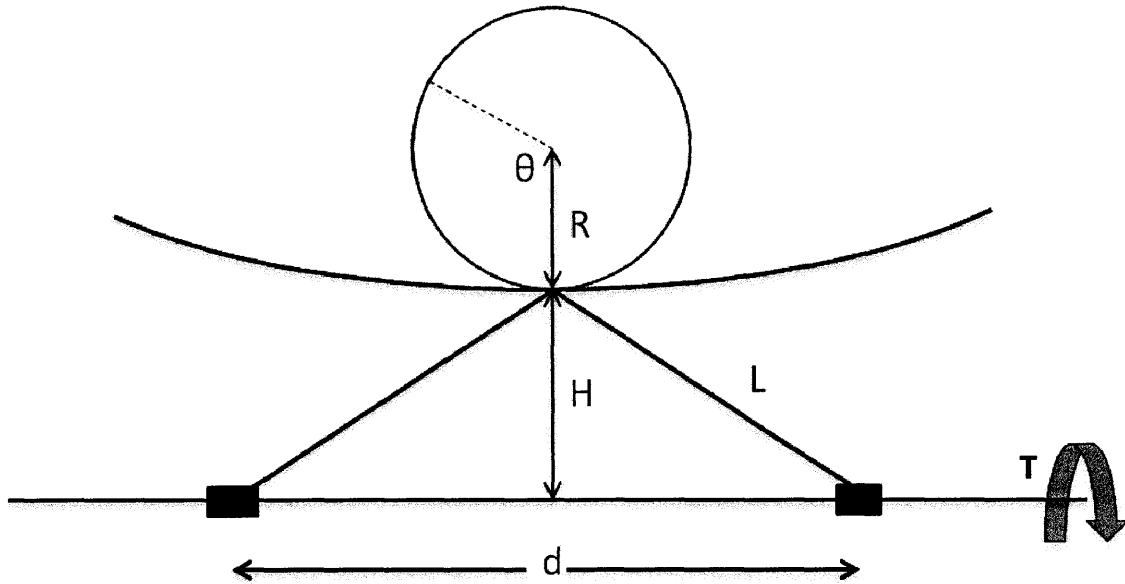


Figure 10: Visualization of physical dimensions R, H, L, and d used in slider-crank calculations, showing R=focal length.

The first boundary condition dictates that the length of each bar must be at its minimum when the trough is at  $\theta=0$ . This is required for the arms to switch loading. D is the distance between the bases on the lead screw. This distance does not change throughout actuation.

$$d = 2 * \sqrt{L^2 - H^2}$$

The second condition dictates that when the trough is at its maximum deflection of  $110^\circ$  the driving arm is vertical.

$$L = H + R[1 + \sin(20^\circ)]$$

Lastly, the total length of the lead screw can be calculated by adding the spacing distance to the base locations at  $110^\circ$  and  $-110^\circ$  degrees.

$$d_{tot} = 2 * [d + R\cos(20^\circ)]$$

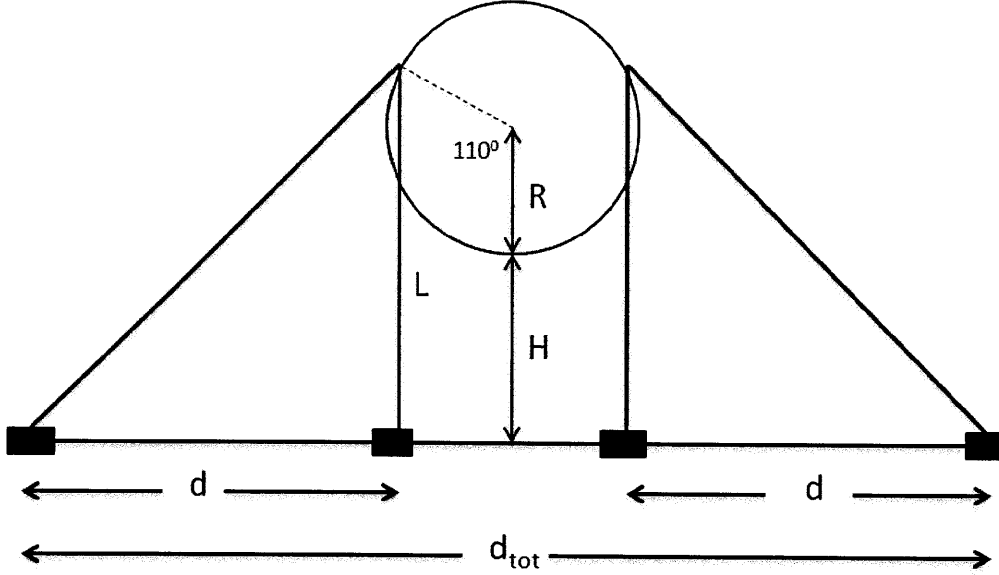


Figure 11: Second boundary condition, where the driving arm is vertical, and the case to show the total length of lead screw for slider-crank concept.

### 3.2.3 Analysis and Optimization

A script was written to plot three dimensional response surfaces of screw length, maximum torque and a number of other properties across varying combinations of R and H. This allowed us to see the repercussions of varying components. Since there is not any equation to calculate the cost over varying dimensions, the plots were used to find a balance between lead screw length and motor torque to be paired with parts we know are available to us.

The torque required by each lead screw is given by the following equation using the compressed arm length L, the angle of the trough  $\theta$ , the efficiency of the motor  $\eta$ , the torque required to move the trough  $\Gamma(\theta)$ , the screw lead  $l$ , H and R. The factor of  $\frac{1}{2}$  takes into account one motor per end of the trough.

$$\tau_m(\theta) = \frac{1}{2} * \frac{\Gamma(\theta) * l}{2\pi\eta \left[ \frac{H + R(1 - \cos\theta)}{L} R \cos \left( \theta - \sin^{-1} \left( \frac{H + R(1 - \cos\theta)}{L} \right) \right) \right]}$$

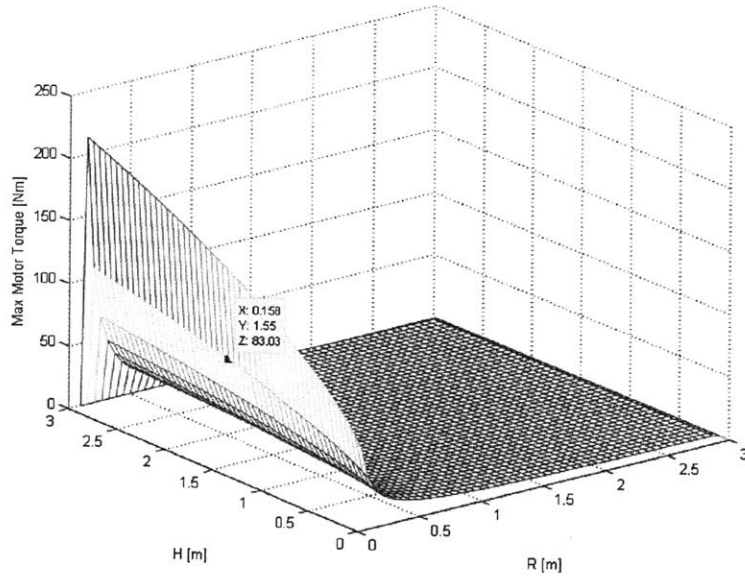


Figure 12: Torque response surface shows the maximum torque throughout the entire 110<sup>0</sup> cycle for any given pair of R and H. Highlighted is the chosen value of approximately R=0.16m and H=1.55m resulting in a maximum torque of approximately 83 Nm assuming a lead of 5 threads/inch and  $\eta=0.5$ .

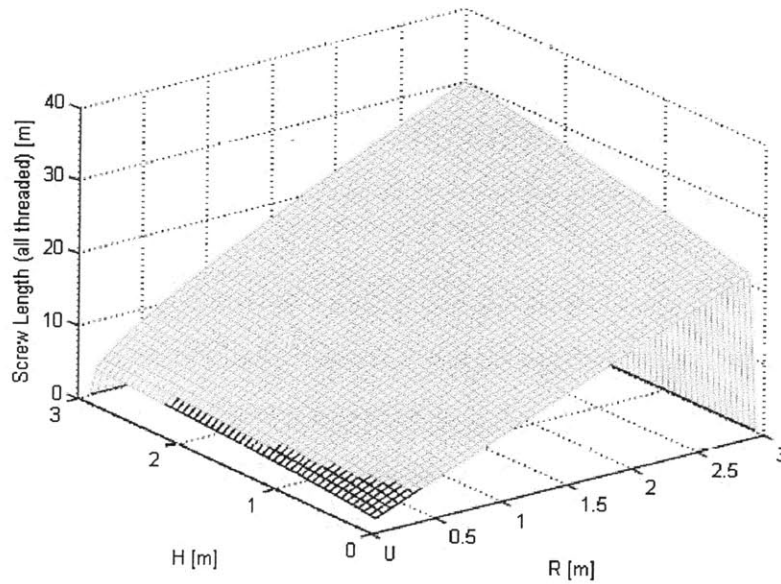


Figure 13: Screw length response surface using the same parameters as above. The color transition shows the boundary between combinations of R and H that make the screw length greater and less than 12ft (3.6m).

In choosing the ideal combination of R and H, the primary factors were max motor torque and lead screw length because they are the largest cost drivers of the actuation system. The values chosen for the prototype model were a 0.16m radius and a height of 1.55m. One of the main reasons for this selection is because the longest available lead screw available outside of custom orders was 12 feet. This combination of R and H required a screw length of 12 feet while still keeping the motor torque down to a reasonable level.

To facilitate testing, the motor will be spec'd to rotate the trough from 0° to 110° in three minutes. Using a lead of 10 rotations/inch, an efficiency of 50% and other calculated values, a setup with a lead screw on each end of the trough (to minimize losses from the parabola torqueing) would require a 0.7 horsepower (no safety factor) motor at either end of the trough 4m prototype trough.

### **3.2.4 Primary Failure Modes**

#### Lead Screw Locking Up

This is the case in which the lead screw becomes jammed. The two main instances when this would happen is if the lead screw buckles, causing misalignment with the screw coupling, or if debris becomes caught in the threads. To minimize the problem of buckling, the lead screw root diameter was chosen to have a safety factor of 2 with respect to the buckling loads of the given trough properties. To prevent the lateral guide from becoming misaligned and locking up the system, it was designed with wheels that would keep it in line and the connection between the lead screw and the arm was designed to only translate an axial load onto the screw. This design is covered in sections 3 and 4 of this paper. In the second case we would ideally like to design to minimize the amount of debris that might get on the screw. This is why the prototype design has the screw located below the I-beam, protecting it from some of the falling particulates.

## Arm Bases out of Sync

This failure mode is most easily solved by using a controller as opposed to simply assuming that applying equal currents will drive the screws at the exact same speed. Depending on the wear and condition of the screw, frictional forces can slow one screw more than the other. Testing of the full scale model will tell us more about how prevalent this problem will be. If it is negligible throughout one cycle, having each end's mechanism zero itself to a known position with a switch every night might be a cheap and easy solution. If it poses problems throughout the day, each end of the trough may have to be controlled separately.

### **3.3 Twin Four-Bar Concept**

#### **3.3.1 Description**

This design concept uses two actuators per end to force the trough around its focal point. Figure 14 shows an example of one of the mechanical linkages in the system. Instead of having a single fixed arm like most four-bar linkages, it has two fully constrained supports. These would be built in to the support structure, most likely the kingpost and base. An arm of fixed length would be allowed to rotate radially about the focal point. The last arm consists of an actuator, most likely driven by a ball screw as will be discussed in a further section.

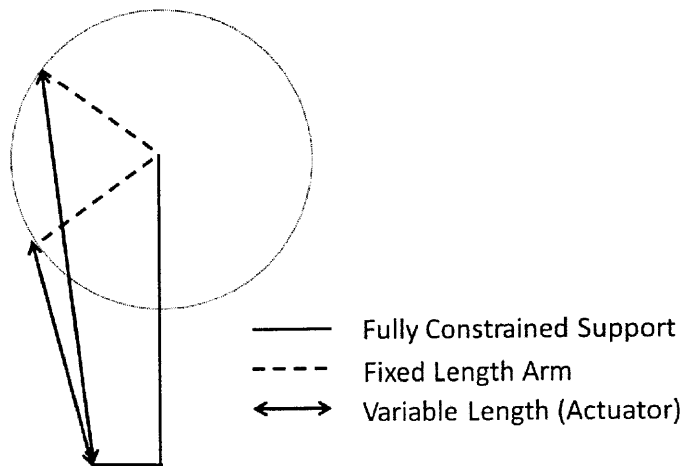


Figure 14: A general illustration of the twin four-bar concept.

The full system would include four actuators, two on each end working in tandem in a push-pull system. The second would be a mirror image of the arm shown in Figure 14. With four arms, there will be no singularities when the trough is actuated between -110 and 110 degrees. By adjusting the lengths of the fixed arms, the mechanical advantage can be manipulated to minimize the power requirements of the system.

### 3.3.2 Geometric Analysis

As compared to the slider crank, which has one constraining arm, the twin four-bar system has two arms that continuously change as the trough rotates. The initial variables are shown in Figure 15 where  $H$  is the vertical distance between the fixed ring of rotation (the black circle) and the level where the actuators are based,  $R$  is the radius of the fixing point's path (not necessarily the focus length),  $\beta$  is the angle from the center of the trough that the fixing point is placed, and  $D_A$  is the horizontal distance between the base of the actuator and the focal point.  $L_A$  is the length of the actuator and is dynamic as the trough rotates.

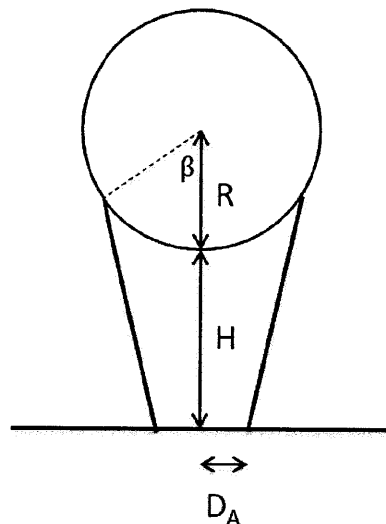


Figure 15: Visualization of physical dimensions  $R$ ,  $H$ ,  $D_A$  and  $\beta$  used in twin four-bar concept calculations.

The following calculations will be for the left actuator of an end. The calculations for the right end are similar with slightly different trigonometric relations.

As the trough moves, the fixing point's coordinates can be described, where  $\varphi$  is the clockwise rotational angle of the trough.

$$P_x = D_A - R\cos(\beta - \varphi)$$

$$P_y = H + R\sin(\beta - \varphi)$$

Through a number of trigonometric relations, the net lever arm of the actuator with respect to the focal length becomes:

$$LA_L = \sin \left[ \tan^{-1} \left( \frac{H + P_y}{D - P_x} \right) \right]$$

In a push pull system, each lever arm can provide the same amount of applied force to aid the rotation of the trough. Therefore, to minimize the maximum force required by the actuators at any given time, they would all apply the same force. Therefore:

$$F_{max} = \frac{\text{Required Torque}}{\text{Net Positive Leverarm}}$$

### 3.3.3 Actuator Speed and Length

An important issue with this design is how the actuators do not move at the same rate. That means that they either have to be controlled separately or must be back drivable so that the system does not lock up if one gets ahead of the other. Figure 16 shows the velocity of each actuator using an arbitrary combination of the defining variables. It clearly shows that the actuators must travel at different speeds and directions to allow this mechanism to function. This observation must be taken into account when making the final design choice.



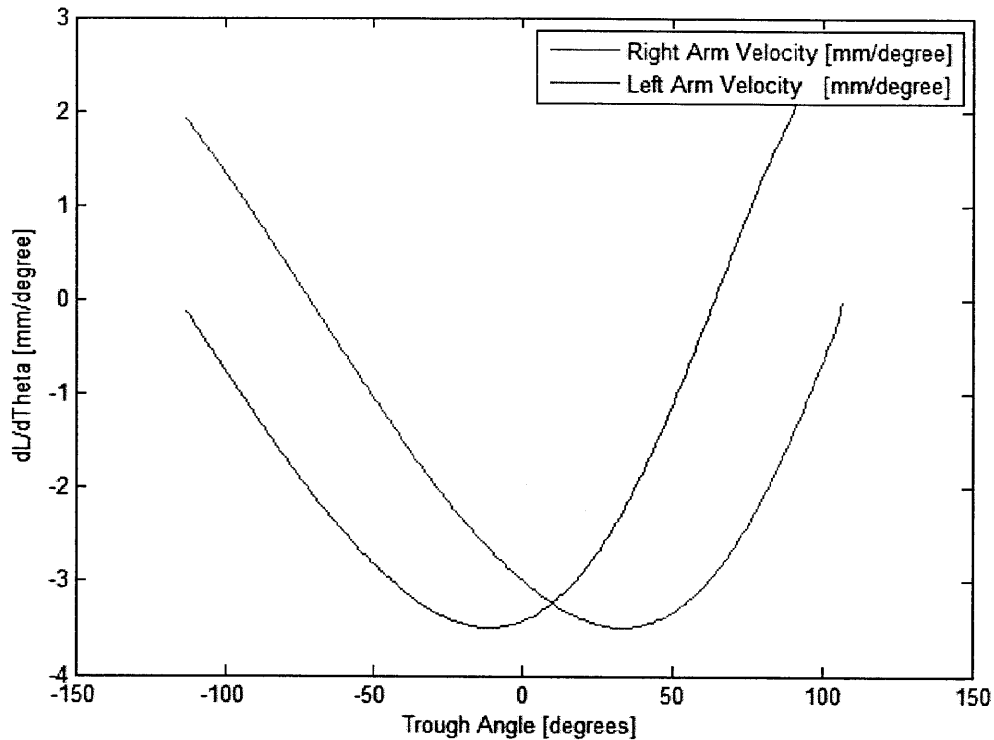


Figure 16: Actuator velocity vs. trough angle for the twin four-bar actuators.

### 3.3.4 Analysis and Optimization

When initially evaluating this concept we looked into using hydraulic and ball screw actuators. Response surfaces were created to assess the ideal values for the height, radius and spacing distance. When costing actuators, the stroke length and compressed length are important to look at. Generally, actuators cannot effectively extend more than 80% of their compressed length. Figure 17 shows only compression ratios and compressed lengths for combinations resulting in maximum ratios of 1.8 and minimum ratios of 1.3. This results in situations when the actuator is used to its potential but not past it. For these figures the base distance was automatically set to maximize force when the trough reaches 60 degrees, where the required torque reaches its maximum due to wind torque and gravity.

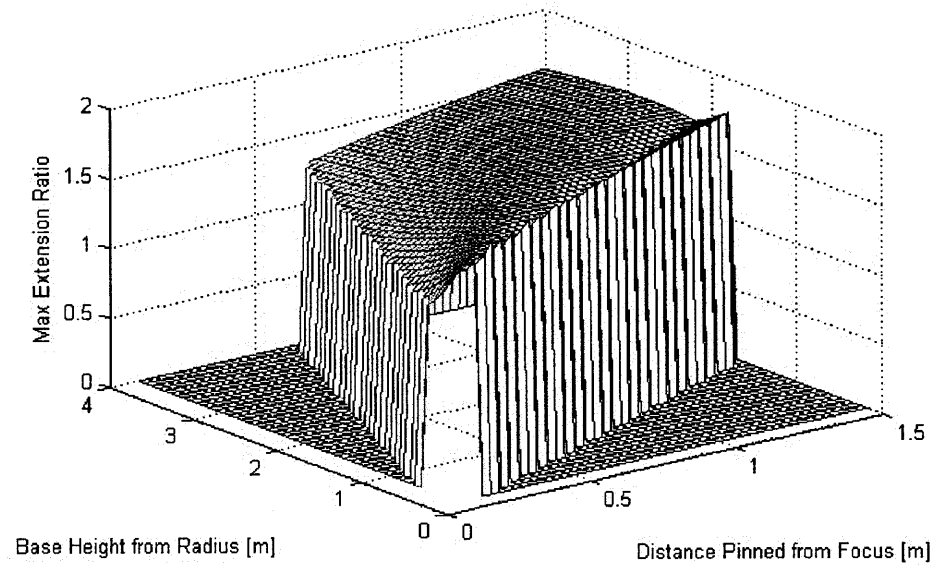
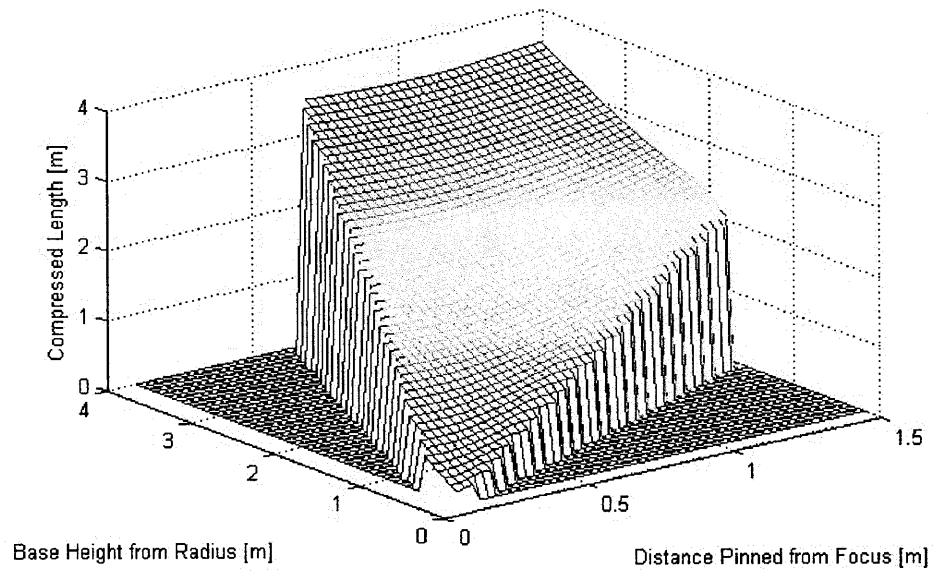


Figure 17: Twin four-bar actuator lengths and compression ratios only shown for ratios between 1.3 and 1.8. Theta=35.

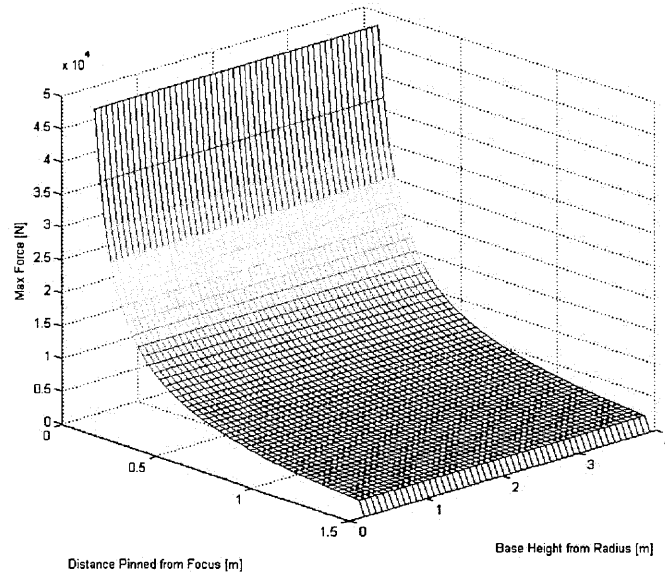


Figure 18: Twin four-bar force response surface showing that the maximum force required to rotate the trough increases exponentially as the pinned point approaches the center of the trough. Theta=35 degrees.

The response surfaces for the twin four-bar clearly favor lower values of R and H when it comes to costing the actuators and favors using a larger diameter when costing driving force for the actuators.

After discussing the options for driving the actuators, we settled on using ball screw actuators. Hydraulics tend to leak, and the manifolds, hoses, and pumps are expensive and require constant maintenance. Ball screws are not cheap, but they do not require linked pressure hose systems. The primary draw of ball screw actuators was the fact that they are backdrivable. This means that if an arm is out of position from where it should be, one of the actuators would backdrive itself instead of locking up and potentially destroying the entire system.

### **3.3.5 Primary Failure Modes**

#### Actuators out of Phase

The primary failure mode of this system is the case where one actuator becomes out of sync with the others. This immediately halts the entire system, putting undue stress on all the joints. This could possibly reach a destructive level if the structure is not built to withstand those forces. The primary solution for this problem is a controls system that monitors the length of each screw at any given time. If this fails, the result is catastrophic and could cost the entire price of the trough. This failure mode is one of the primary reasons this system was not selected for the final design.

#### Hydraulic Fluid or Air Leak

If the option of hydraulic or pneumatic cylinders were pursued, the system runs the risk of leaking fluid. This failure mode is not catastrophic, but would be costly in maintenance in the long run after continual care. Each failure requires the individual trough to be taken out of service with possible others depending on the design of the system's shutoff valves.

## **3.4 Manufacturing Design and Costing**

### **3.4.1 Slider Crank Manufacturing Design**

The proposed manufacturing plan for the 4 meter prototype is to use a single lead screw and motor per end of the trough. The base of each arm would be constrained by a customized I-beam trolley driven along an I-beam. This would allow the design to utilize mostly ready-to-order parts, simplifying the prototype process which is the primary goal at this stage of the project. The only custom parts would be the bottom clevis and the block used to couple the lead screw to the trolley and clevis.

Figure 19 shows the entire slider crank mechanism. A number of parts are hidden or were not implemented in this model but will be in the final design. Figure 20 shows a closer rendering of the trolley mechanism, which replaces the traditional loop at the bottom with the coupling mechanism. This mechanism places the clevis attachment in line with the screw coupling to prevent the lever arm from creating a net moment. In this design the I-beam will ideally bear the entire vertical force while the screw will bear the entire horizontal force. Future analysis into the roller friction will take place once the design is further refined to ensure the torque is minimized.

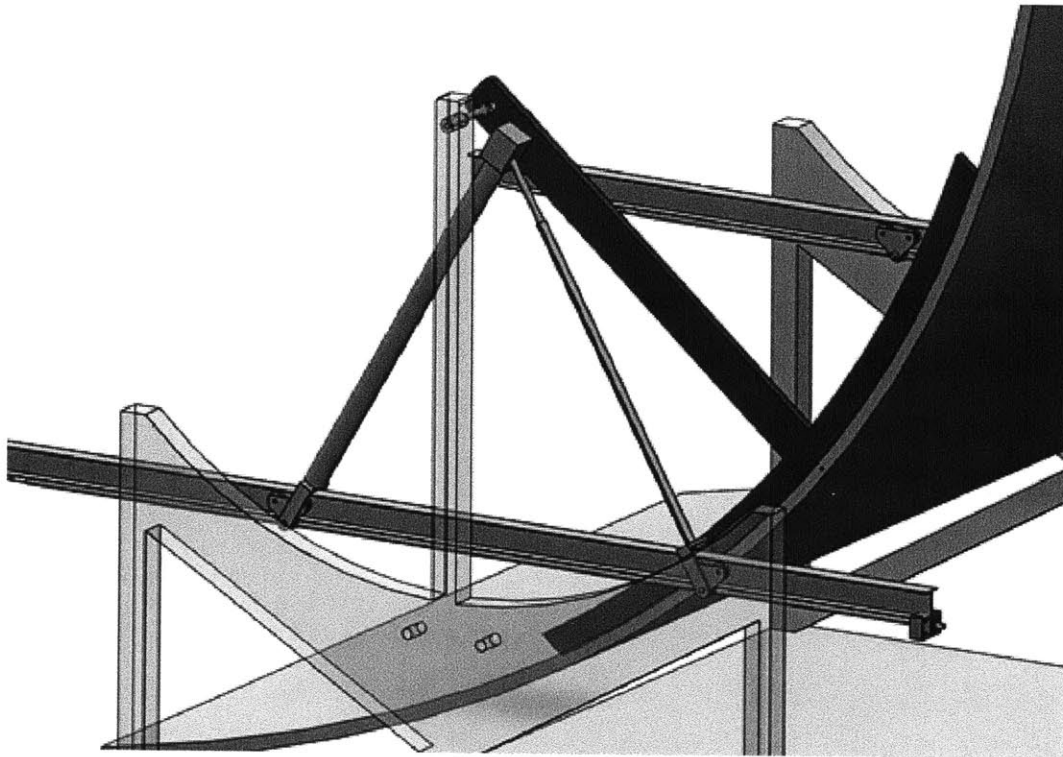


Figure 19: Simple SolidWorks model of the slider crank concept. At this point the left arm is driving the trough while the right arm extends.

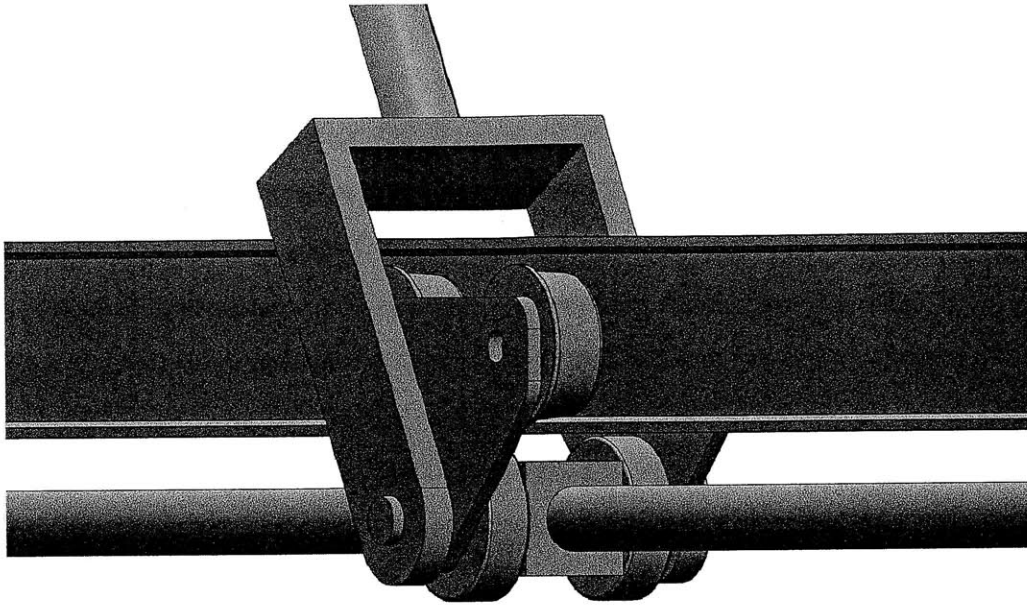


Figure 20: Example of the slider crank trolley acting as a linear guide on an I-beam.

### 3.4.2 Twin-Four Bar Manufacturing Design

The proposed manufacturing plan would be to use two ball screw actuators per end. As shown in the failure mode analysis of this design, the actuators must move at different rates. This necessitates either an accurate controls system or a back drivable actuator. Since the controls system leaves too high of a chance of malfunctioning, we concluded that using ball screws would be the most logical option. If the actuator motors were driven at a constant current, the screw that must move faster to keep up will simply allow the motor to spin more quickly. If it cannot keep up still, the ball screw can simply back drive itself along the screw so it does not lock up the entire system. The screw couplings are very costly, as can be seen in the cost table, making this design the less desirable of the two considered.

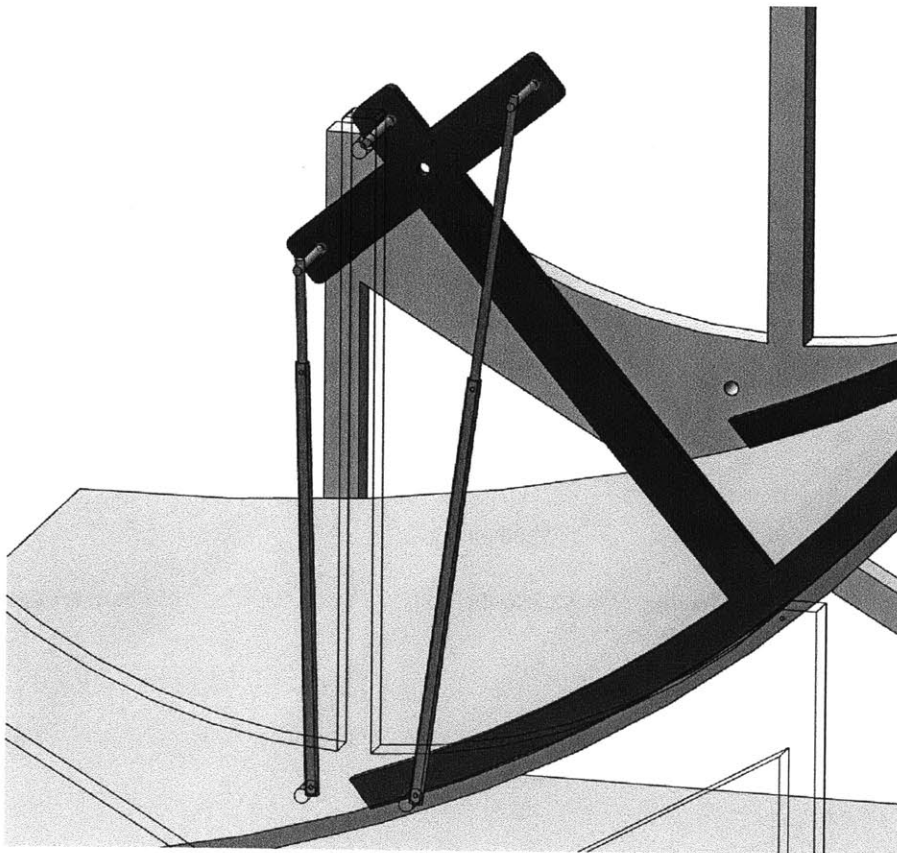


Figure 21: Close up of a rough SolidWorks model of the twin four bar design.

### 3.4.3 Preliminary Cost Comparison

Quantity: 1 Trough

#### I-Beam Slider Crank

Part Name	Qty	Total
<b>Linkage System</b>		<b>\$405.80</b>
Top Clevis	4	\$80.48
Solid Rod End	2	\$37.04
Clevis Pins	0	\$0.00
Arm, Outer Pipe	4	\$207.24
Arm, Inner Pipe	4	\$81.04
<b>Drive System</b>		<b>\$349.56</b>
Motor	2	\$254.14
Lead Screw Coupling	2	\$36.68
Fasteners	-	\$29.37
Anchors	2	\$15.06
Nuts	1	\$14.31
<b>Linear System</b>		<b>\$1,495.52</b>
Lead Screw	2	\$154.00
I-Beam	2	\$220.00
Shaft Bearings	4	\$141.52
Beam Supports	4	\$160.00
Bottom Clevis	4	\$140.00
I-Beam Trolley	4	\$480.00
Trolley		
Customization	4	\$200.00
<b>Cost/Trough:</b>		<b>\$2,250.88</b>

#### Twin Four Bar

Part Name	Qty	Total
<b>Linkage System</b>		<b>\$594.64</b>
Clevis	8	\$160.96
Clevis Pins	8	\$19.20
Outer Pipe	8	\$414.48
<b>Drive System</b>		<b>\$626.07</b>
Motor	4	\$508.28
Coupling	4	\$73.36
Anchors	4	\$30.12
Nuts	1	\$14.31
<b>Linkage Drive</b>		<b>\$1,903.48</b>
Ball Screw	4	\$247.92
Ball Screw Mount	4	\$1,655.56
<b>Cost/ Trough:</b>		<b>\$3,124.19</b>



## IV. Final Design and Full Scale 4m Prototype

### 4.1 Selection of Slider Crank

Primarily for cost reasons, the slider crank concept has been chosen to be built at full scale on the test trough currently in New Hampshire. The design requires fewer and lower powered motors and does not use expensive ball screws. This saves in cost, maintenance, and energy usage throughout its lifetime. Lastly, the materials are less reliant on precision than the twin four-bar design. Ball screws are expensive and will most likely be more difficult to source from local areas.

### 4.2 Improved Slider Crank Design

During the final days of this project, the design team decided to use a modified version of the slider crank design in the full scale prototype. Since the two trolleys are spaced equally at all times, we are planning on fixing them together with a rigid connection and only having one of the trolleys attached to the lead screw. This improved design allows affords a number of advantages over the original. An illustration of this and the system can be seen in Figure 22.

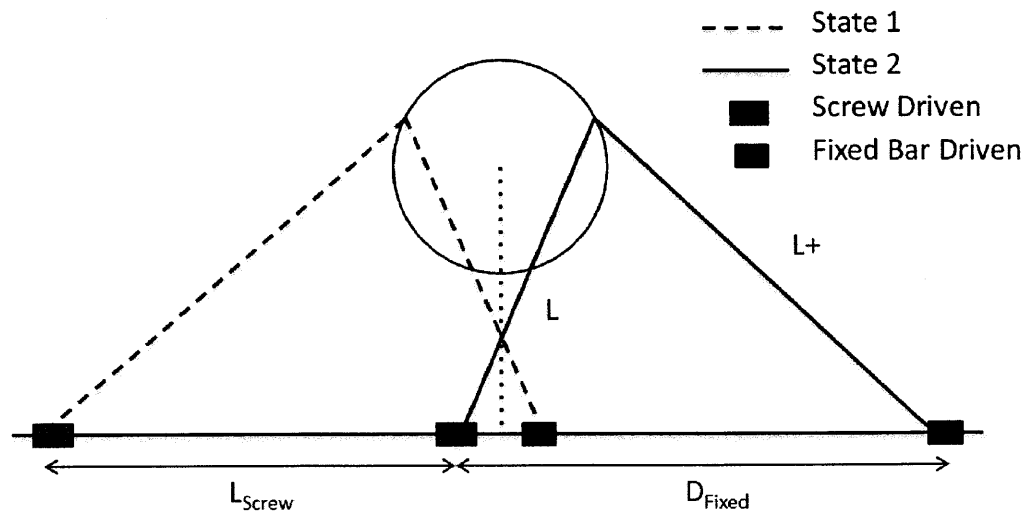


Figure 22: Illustration of the improved slider crank design at -110 and 110 degrees employing a fixed connection of length  $D$  to link the two trolleys and a shorter screw of length  $L$ .

The first advantage is that it allows for the use of a shorter lead screw. The primary reason for this is because it only has to span the travel distance of one trolley. A shorter screw means a lower overall system costs as well as an increased maximum buckling load for any given screw diameter. Depending on the required screw length chosen, the screw diameter could be decreased to drop costs even further. The only increase in cost due to this is the linkage would be low cost steel.

A second advantage is if the geometric parameters are set to not have either trolley roll past the center point of the trough, the I-beam linear guide can be supported at the center, halving the distance of unsupported beam. This will greatly decrease the maximum beam deflection and could possibly allow for cost savings from using a smaller overall beam. This configuration requires the arms to be longer, which decreases the length of lead screw needed to actuate the trough's full range.

The third advantage is that for the final design, by only having one trolley attached to the screw and having neither pass the center of the trough, it will be easier to shield the screw from the elements such as sand and moisture. The final design will most likely employ a telescoping tube design to completely encase the lead screw and its lubricants to improve the lifespan of the system.

The last main advantage is that by shortening the required lead screw, it relaxes the constraint of only having 12 foot screws available. This allows us to consider a wider range of R and H. The new dimension possibilities open up the option of increasing R, decreasing the axial load and strain on the various joints in the assembly or increasing H, which would decrease overall shading. Response surfaces of the lead screw length and motor torque, respectively, can be seen in Figures 23 and 24. Figure 23 only shows combinations using lead screws less than 12ft. The improved selection of R and H combinations compared to those limited to a 12m screw using the old design is clear when comparing Figures 13 and 23.

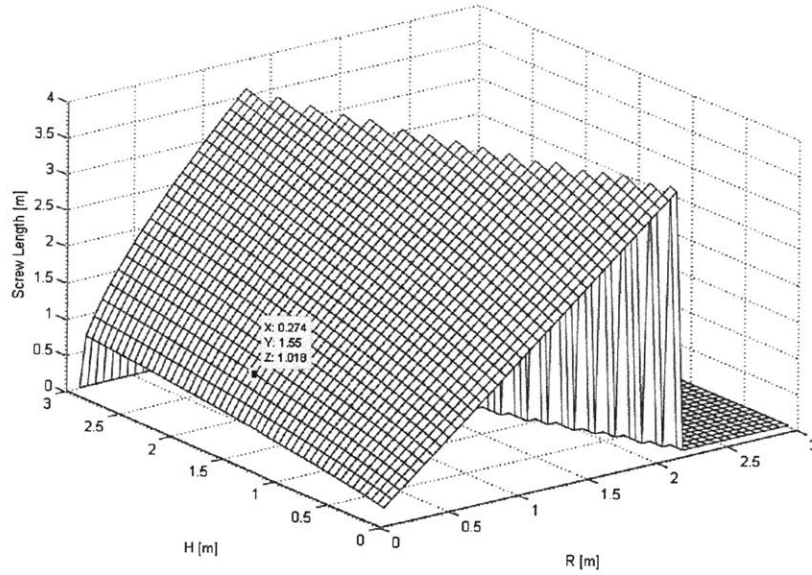


Figure 23: Response surface for the improved slider crank design using the case where the trolley reaches 0.2m from the center of the trough. A screw length of 1.02m is required in the case where H=1.55m and R=0.274m which will be used in the 4m trough prototype. Showing only values less than 12ft.

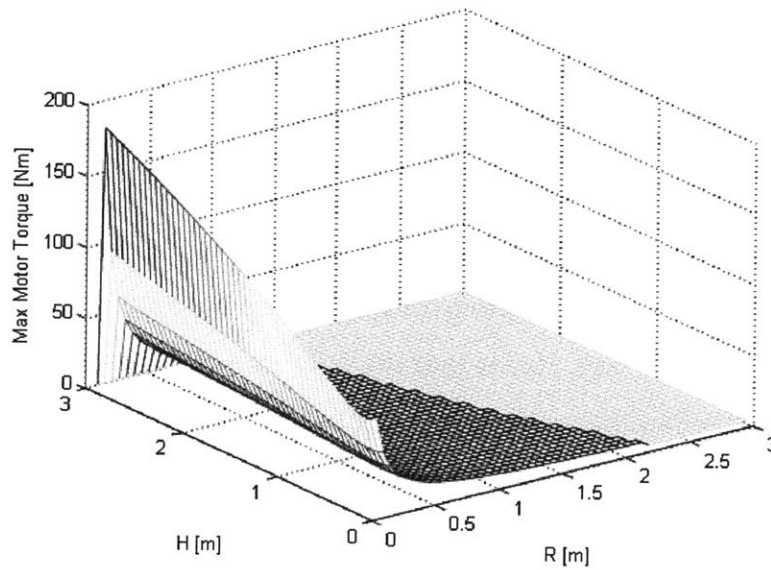


Figure 24: Torque response surface for the improved slider crank design using the case where the trolley reaches 0.2m from the center of the trough. A maximum of 32Nm of torque is required for the parameters chosen for the prototype trough (R=0.274m, H=1.55m).

The values of R and H chosen for the prototype design are  $R=0.274\text{m}$  and  $H=1.55\text{m}$ . These resulted in a lead screw length of approximately 1m, a maximum torque of 32Nm, and requiring 0.08 horsepower motors (without any safety factor) at either end of the trough. The primary reason for not increasing R and H too much was because as each goes up, the total length of the trolley system increases. Using these values, the linear guide length will be approximately 16 feet. This is the one downside of the new design. It will require slightly more materials from the length of the arms as well as the I-beam. Even so, those costs will be less than that saved on the shorter lead screw, one less coupling device, and costs of more complicated or less effective protective devices. Due to the longer arms, it will also have a slightly higher axial load because the arms will be at a lower angle from horizontal at any given time than the old design, but the decreased length of the lead screw makes this easier to manage.

### **4.3 Part Design and Selection**

#### **4.3.1 Linear Guide**

As described in the previous section, the linear guide will be made using an I-beam and an I-beam trolley. The trolleys will be customized by replacing the standard bar at the bottom normally used to hang loads, one with the lead screw coupling and the other with a coupling for the rigid connection. Each will add a clevis attachment point. This means that the only custom made pieces for the guide are the new trolley coupling mechanism and the large clevis that is needed to reach above the I-beam. As described in section 4.2, the I-beam will be supported at its ends as well as in the center.

#### **4.3.2 Screw Coupling**

The screw coupling designed for the New Hampshire prototype will look something like Figure 25, which shows half of the trolley assembly with the coupling block at the bottom. The main center hole is where the part couples with the lead

screw. It is machined out of a single block that supports two pins. Mounted on those pins will be first, starting from the inside, a wheel to keep the trolley from moving vertically when the actuator arms are extending, second the trolley frame, and third the bottom clevis. The outer flange supports the pin so it can bear the full load of the trough. The bottom flange of the I-beam is situated in between the top set and bottom wheel while the top flange is just above the top pair of wheels.

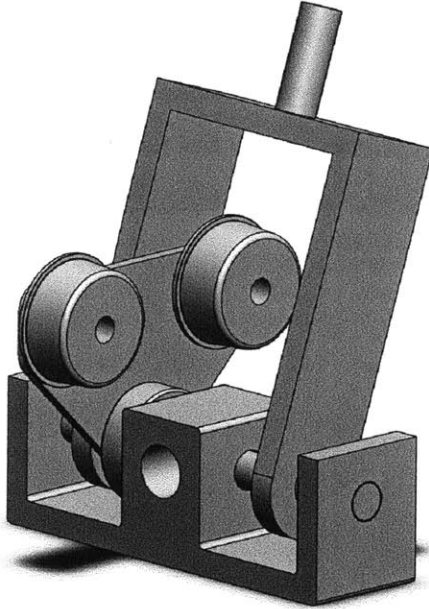


Figure 25: Preliminary custom screw coupling for slider crank design shown with half of the trolley assembly.

#### 4.3.3 Other Couplings and Materials Selection

The couplings for the motor and lead screw as well as the lead screw mounts are being designed by my teammates, Eric Gilbertson and Tim Robertson. Their materials selection and analysis will be contained in the final project report to be given for the 2.752 presentations and Eni's evaluation. Parts are currently ordered to be sent to MIT and New Hampshire to be built onto the existing 4 meter prototype.

## **V. Further Work**

At the time of publishing, parts for the improved slider crank design have been ordered and shipped to MIT and New Hampshire to be assembled in the coming weeks. It will be used to assess possible failure modes and design flaws that have not yet been discovered. It will also give a good assessment of the accuracy of the system and a better understanding of how the frictional forces and backlash will factor into the final product. These experiments as well as further design refinement of the trolley and motor systems will all factor into the final design. Lastly, Professor Campbell is to meet with the Eni liaison later in the month to present updates on this work and other parts of the overall trough design process.

## VI. References

- [1] *MIT ENI Presentation Slides\_10-Stacy 6-29-10.key.pdf*, June 2010, unpublished material.
- [2] Ziegenhagen. *20100412 Trough*, April 2010, unpublished material.
- [3] Elamouri, Amar, "Wind Energy Potential in Tunisia," *Renewable Energy* Volume 33, Issue 4, April 2008, Pages 758-768.
- [4] Bowden, S. and Honsberg, C. *PVEducation.org*. Solar Power Labs at Arizona State University, National Science Foundation, 2010. Web. 14 April 2011.